

NO• Release from MbFe(II)NO and HbFe(II)NO after Oxidation by Peroxynitrite

Susanna Herold* and Francesca Boccini

Laboratorium für Anorganische Chemie, Eidgenössische Technische Hochschule, ETH Hönggerberg, CH-8093 Zürich, Switzerland

Received March 20, 2006

In this work, we showed that the reaction of peroxynitrite with MbFe(II)NO, in analogy to the corresponding reaction with HbFe(II)NO (Herold, S. *Inorg. Chem.* **2004**, *43*, 3783–3785), proceeds in two steps via the formation of MbFe(III)NO, from which NO• dissociates to produce iron(III)myoglobin (Mb = myoglobin; Hb = hemoglobin). The second-order rate constants for the first steps are on the order of 10^4 and $10^3 \text{ M}^{-1} \text{ s}^{-1}$, for the reaction of peroxynitrite with MbFe(II)NO and HbFe(II)NO, respectively. For both proteins, we found that the values of the second-order rate constants increase with decreasing pH, an observation that suggests that HOONO is the species responsible for oxidation of the iron center. Nevertheless, it cannot be excluded that the pH-dependence arises from different conformations taken up by the proteins at different pH values. In the presence of 1.2 mM CO₂, the values of the second-order rate constants are larger, on the order of 10^5 and $10^4 \text{ M}^{-1} \text{ s}^{-1}$, for the reaction of peroxynitrite with MbFe(II)NO and HbFe(II)NO, respectively. The pH-dependence of the values for the reaction with MbFe(II)NO suggests that ONOOCO₂⁻ or the radicals produced from its decay (CO₃^{•-}/NO₂[•]) are responsible for the oxidation of MbFe(II)NO to MbFe(III)NO. In the presence of large amounts of nitrite (in the tens and hundreds of millimoles range), we observed a slight acceleration of the rate of oxidation of HbFe(II)NO by peroxynitrite. A catalytic rate constant of $40 \pm 2 \text{ M}^{-1} \text{ s}^{-1}$ was determined at pH 7.0. Preliminary studies of the reaction between nitrite and HbFe(II)NO showed that this compound also can oxidize the iron center, albeit at a significantly slower rate. At pH 7.0, we obtained an approximate second-order rate constant of $3 \times 10^{-3} \text{ M}^{-1} \text{ s}^{-1}$.

Introduction

Nitrogen monoxide generated from the endothelial isoform of nitric oxide synthase (eNOS)¹ plays an important role in vascular homeostasis by dilating the blood vessels and by regulating blood cell adhesion.² These functions are mediated by the interaction of NO• with cells of the vascular wall. However, a large part of NO• produced by eNOS reacts with blood components, in particular, with hemoglobin (Hb). Because of the large values of the second-order rate constants of the reactions of NO• with oxyHb and deoxyHb (both on

the order of $10^7 \text{ M}^{-1} \text{ s}^{-1}$),^{3–5} it has been proposed that Hb is the main sink of NO• in the blood. It has recently been shown that, upon inhalation of 80 ppm NO•, iron(III)hemoglobin (metHb) reaches a concentration approximately 60 times higher than that of HbFe(II)NO.⁶ Thus, most inhaled NO• reacts with oxyHb to produce the bioinactive compound nitrate, and only a minor fraction binds to deoxyHb, as expected from the relative concentrations of the two Hb species.

In contrast to these experimental results, it has been proposed that NO• may be transported in the vasculature via the formation of a rather stable S-nitroso adduct of the cysteine residues β93 of Hb. According to this highly criticized hypothesis,^{7–9} the formation of SNO–Hb proceeds

* To whom correspondence should be addressed. Tel.: (41)(44) 632 28 58. Fax: (41)(44) 632 10 90. E-mail: herold@inorg.chem.ethz.ch.

(1) Abbreviations: eNOS, endothelial nitric oxide synthase; Hb, hemoglobin; HbFeO₂, oxyhemoglobin (oxyHb); HbFe(II)NO, nitrosyl-hemoglobin; metHb, iron(III)hemoglobin; HbFe(IV)=O, oxoiron(IV)-hemoglobin (ferrylHb); Mb, myoglobin; MbFeO₂, oxy-myoglobin (oxyMb); MbFe(II)NO, nitrosylmyoglobin; metMb, iron(III)myoglobin; MbFe(IV)=O, oxoiron(IV)myoglobin (ferrylMb); HbFe(II), deoxyhemoglobin (deoxyHb); SNO–Hb, hemoglobin tetramer with both Cysβ93's S-nitrosated.
(2) Palmer, R. M. J.; Ferrige, A. G.; Moncada, S. *Nature* **1987**, *327*, 524–526.

(3) Eich, R. F.; Li, T.; Lemon, D. D.; Doherty, D. H.; Curry, S. R.; Aitken, J. F.; Mathews, A. J.; Johnson, K. A.; Smith, R. D.; Phillips, G. N., Jr.; Olson, J. S. *Biochemistry* **1996**, *35*, 6976–6983.
(4) Herold, S.; Exner, M.; Nauser, T. *Biochemistry* **2001**, *40*, 3385–3395.
(5) Cassoly, R.; Gibson, Q. H. *J. Mol. Biol.* **1975**, *91*, 301–313.
(6) Pikhova, B.; Gladwin, M. T.; Schechter, A. N.; Hogg, N. *J. Biol. Chem.* **2005**, *280*, 40583–40588.

via the transfer of the so-called NO-group¹⁰ from the heme [HbFe(II)NO] to Cys β 93.^{11–13} In addition, it has recently been shown that deoxyHb reacts with nitrite, a major product of NO \cdot metabolism in blood,¹⁴ to regenerate NO \cdot as well as HbFe(II)NO.^{14–16} Clearly, several mechanisms exist in vivo to produce HbFe(II)NO. However, the amount of HbFe(II)NO present under physiological conditions is still a matter of debate: <1 nM,⁹ <200 nM,⁶ 0.2–0.4 μ M,¹⁷ and 1.25–5 μ M¹⁸ are some of the values found in the literature. Moreover, it is unclear whether NO \cdot can be released from HbFe(II)NO and thus whether its bioactivity may be recovered.

Recent studies have shown that upon inhalation of 80 ppm NO \cdot the venous HbFe(II)NO concentration was generally lower than the arterial concentration and that the half-life of HbFe(II)NO in vivo is \sim 40 min.⁶ This rather long half-life may suggest that, after interruption of NO \cdot inhalation, HbFe(II)NO formation continues, possibly by the reaction of deoxyHb with nitrite, which is also produced upon NO \cdot inhalation.⁶ As NO \cdot dissociation from HbFe(II)NO is a very slow process ($t_{1/2}$ < 11 min),^{19,20} in order to utilize the bioactivity of NO \cdot , it is likely that in vivo NO \cdot is liberated by an alternative mechanism. One possible pathway for NO \cdot release from HbFe(II)NO may involve oxidation of the iron center followed by the significantly faster NO \cdot dissociation from HbFe(III)NO ($t_{1/2}$ < 1 s).^{21,22}

Myoglobin (Mb), the monomeric hemoprotein present in cardiac, skeletal, and smooth muscle,^{23,24} has also been

proposed to play an important function in regulating the NO \cdot concentration in these tissues. In analogy to Hb, both oxyMb and deoxyMb can scavenge NO \cdot . In addition, it has recently been demonstrated that MbFe(II)NO is formed in ischemic hearts, in particular, in the presence of high nitrite concentrations.²⁵ Upon reperfusion of the hearts, the concentration of MbFe(II)NO decreased, an observation that suggests that MbFe(II)NO may also represent a form to store NO \cdot .²⁵

We have previously shown that peroxyxynitrite²⁶ can oxidize the iron center of HbFe(II)NO to produce HbFe(III)NO, from which NO \cdot dissociates to generate metHb.²¹ A similar reaction was recently observed upon the reaction of HbFe(II)NO with NO $_2\cdot$ or with carbonate radicals [CO $_3\cdot^-$, systematic name: trioxidocarbonate (\bullet 1–)].²⁷ In the present study, we report mechanistic studies of the reaction of peroxyxynitrite with MbFe(II)NO as well as with HbFe(II)NO under various experimental conditions. We show that the pH-dependence of the second-order rate constants indicates that HOONO and NO $_2\cdot$ /CO $_3\cdot^-$ are the species responsible for oxidation of the iron center, in the absence and in the presence of CO $_2$, respectively. High concentrations of nitrite catalyze the peroxyxynitrite-mediated oxidation of HbFe(II)NO, possibly by forming an adduct with HOONO that is more reactive than peroxyxynitrite. Finally, we show that nitrite can also bring about the oxidation of MbFe(II)NO and HbFe(II)NO to their corresponding iron(III) forms, though at a significantly slower rate.

Experimental Section

Reagents. All chemicals used were of the highest purity available. Sodium bicarbonate was purchased from Merck and sodium nitrite from Fluka. Horse heart metmyoglobin was purchased from Sigma. Purified human oxyHb stock solution HbA $_0$ (57 mg/mL solution with approximately 1.1% metHb and no apoHb) was a kind gift from APEX Bioscience, Inc. (NC). Nitrogen monoxide was obtained from Linde and passed through a NaOH solution as well as a column of NaOH pellets to remove higher nitrogen oxides before use. Aqueous NO \cdot -saturated solutions (2 mM) were prepared as described previously.²⁸ For the preparation of the MbFe(II)NO solutions, NO \cdot was purified by passing it first through a NaOH solution and then through two traps cooled with dry ice/2-propanol to condense residual traces of N $_2$ O $_3$ still present in the line.

Peroxyxynitrite, Carbon Dioxide, Nitrite, and Protein Solutions. Peroxyxynitrite was prepared from [N(CH $_3$) $_4$]O $_2$ and gaseous nitrogen monoxide according to the literature²⁹ and stored in small aliquots at -80 $^{\circ}$ C. Peroxyxynitrite solutions prepared by following this procedure contain significantly lower amounts of nitrite contaminations^{30,31} than those present in solutions made from KO $_2$ and gaseous

- (7) Xu, X.; Cho, M.; Spencer, N. Y.; Patel, N.; Huang, Z.; Shields, H.; King, S. B.; Gladwin, M. T.; Hogg, N.; Kim-Shapiro, D. B. *Proc. Natl. Acad. Sci. U.S.A.* **2003**, *100*, 11303–11308.
- (8) Hobbs, A. J.; Gladwin, M. T.; Patel, R. P.; Williams, D. L. H.; Butler, A. R. *Trends Pharmacol. Sci.* **2002**, *23*, 406–411.
- (9) Rassaf, T.; Bryan, N. S.; Maloney, R. E.; Specian, V.; Kelm, M.; Kalyanaraman, B.; Rodriguez, J.; Feelisch, M. *Nat. Med.* **2003**, *9*, 481–482.
- (10) Stamler and co-workers use this term to describe an undefined form of NO, either NO \cdot or NO $^+$.^{11–13}
- (11) Jia, L.; Bonaventura, C.; Bonaventura, J.; Stamler, J. S. *Nature* **1996**, *380*, 221–226.
- (12) Stamler, J. S.; Jia, L.; Eu, J. P.; McMahon, T. J.; Demchenko, I. T.; Bonaventura, J.; Gernert, K.; Piantadosi, C. A. *Science* **1997**, *276*, 2034–2037.
- (13) Singel, D. J.; Stamler, J. S. *Annu. Rev. Physiol.* **2005**, *67*, 99–145.
- (14) Gladwin, M. T.; Schechter, A. N.; Kim-Shapiro, D. B.; Patel, R. P.; Hogg, N.; Shiva, S.; Cannon, R. O., III; Kelm, M.; Wink, D. A.; Espey, M. G.; Oldfield, E. H.; Pluta, R. M.; Freeman, B. A.; Lancaster, J. R., Jr.; Feelisch, M.; Lundberg, J. O. *Nat. Chem. Biol.* **2005**, *1*, 308–314.
- (15) Cosby, K.; Partovi, K. S.; Crawford, J. H.; Patel, R. P.; Reiter, C. D.; Martyr, S.; Yang, B. K.; Waclawiw, M. A.; Zalos, G.; Xu, X.; Huang, K. T.; Shields, H.; Kim-Shapiro, D. B.; Schechter, A. N.; Cannon, R. O., III; Gladwin, M. T. *Nat. Med.* **2003**, *9*, 1497–1505.
- (16) Nagababu, E.; Ramasamy, S.; Abernethy, D. R.; Rifkind, J. M. *J. Biol. Chem.* **2003**, *278*, 46349–46356.
- (17) Gladwin, M. T.; Ognibene, F. P.; Pannell, L. K.; Nichols, J. S.; Pease-Fye, M. E.; Shelhamer, J. H.; Schechter, A. N. *Proc. Natl. Acad. Sci. U.S.A.* **2000**, *97*, 9943–9948.
- (18) McMahon, T. J.; Moon, R. E.; Luschinger, B. P.; Carraway, M. S.; Stone, A. E.; Stolp, B. W.; Gow, A. J.; Pawloski, J. R.; Watke, P.; Singel, D. J.; Piantadosi, C. A.; Stamler, J. S. *Nat. Med.* **2002**, *8*, 711–717.
- (19) Herold, S.; Röck, G. *Biochemistry* **2005**, *44*, 6223–6231.
- (20) Azizi, F.; Kielbasa, J. E.; Adeyiga, A. M.; Maree, R. D.; Frazier, M.; Yakubu, M.; Shields, H.; King, S. B.; Kim-Shapiro, D. B. *Free Radical Biol. Med.* **2005**, *39*, 145–151.
- (21) Herold, S. *Inorg. Chem.* **2004**, *43*, 3783–3785.
- (22) Sharma, V. S.; Traylor, T. G.; Gardiner, R.; Mizukami, H. *Biochemistry* **1987**, *26*, 3837–3843.

- (23) Wittenberg, B. A.; Wittenberg, J. B. *Annu. Rev. Physiol.* **1989**, *51*, 857–878.
- (24) Qiu, Y.; Sutton, L.; Riggs, A. F. *J. Biol. Chem.* **1998**, *36*, 23425–23432.
- (25) Tiravanti, E.; Samouilov, A.; Zweier, J. L. *J. Biol. Chem.* **2004**, *279*, 11065–11073.
- (26) The recommended IUPAC nomenclature for peroxyxynitrite is oxoperoxynitrate(1-); for peroxyxynitrous acid, it is hydrogen oxoperoxynitrate. The term peroxyxynitrite is used in the text to refer generically to both oxoperoxynitrates.
- (27) Boccini, F.; Domazou, A. S.; Herold, S. *J. Phys. Chem. A* **2006**, *110*, 3927–3932.
- (28) Herold, S.; Röck, G. *J. Biol. Chem.* **2003**, *278*, 6623–6634.
- (29) Bohle, D. S.; Glassbrenner, P. A.; Hansert, B. *Methods Enzymol.* **1996**, *269*, 302–311.

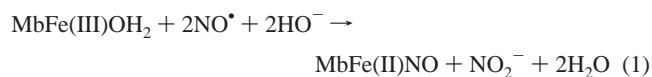
nitrogen monoxide³² and used for the preliminary studies of the reaction between HbFe(II)NO and peroxyntirite.²¹ Indeed, the peroxyntirite solutions contained maximally 10% nitrite relative to the peroxyntirite concentration and no hydrogen peroxide. Nevertheless, nitrite did not interfere with our studies, as the reactions of HbFe(II)NO or MbFe(II)NO with nitrite proceed at a significantly slower rate than the corresponding reactions with peroxyntirite. The peroxyntirite stock solution was diluted with degassed 0.01 M NaOH, and the concentration of the resulting solutions was determined spectrophotometrically prior to each experiment by measuring their absorbance at 302 nm ($\epsilon_{302} = 1705 \text{ M}^{-1} \text{ cm}^{-1}$).²⁹

The 0.1 M phosphate buffers and the 0.01 M NaOH solutions used for all of the experiments were prepared fresh daily and thoroughly degassed. Experiments in the presence of CO₂ were carried out by adding the required amount of a freshly prepared degassed 0.5 M sodium bicarbonate solution to the protein solutions as described in detail in ref 33. The values for the constant of the hydration–dehydration equilibrium $\text{CO}_2 + \text{H}_2\text{O} \rightleftharpoons \text{H}^+ + \text{HCO}_3^-$ were taken from ref 34, by taking into consideration the ionic strength of the solutions. After addition of the bicarbonate solution, the protein solutions were allowed to equilibrate at room temperature for at least 5 min.

The nitrite stock solutions (2 M) used for the investigation of the nitrite-catalyzed reaction between HbFe(II)NO and peroxyntirite were prepared in a 0.1 M K₂HPO₄/NaOH solution. The final pH was approximately 9.5. The 2 M nitrite stock solutions used for the studies of the reaction between HbFe(II)NO and nitrite were prepared in a 0.1 M phosphate buffer. Sodium nitrite was first dissolved in a K₂HPO₄ solution (pH 8.6), and then enough KH₂PO₄ solution (pH 4.6) was added to reach the desired final pH of 7.0–7.3.

For the preparation of concentrated HbFe(II)NO solutions, an ice-cooled oxyHb solution (ca. 1 mM in a 0.1 M phosphate buffer at pH 7.0) was first deoxygenated with a constant flow of Ar over the surface of the solution while gently stirring. Then, approximately 2 equiv of a saturated NO• solution were added to the deoxyHb solution. The excess of NO• was finally removed by purging the solution again with Ar. The final concentration of the diluted HbFe(II)NO solutions used for the kinetics studies was determined prior to each experiment by measuring the absorbance at 544 and 572 nm ($\epsilon_{544} = 11.4 \text{ mM}^{-1} \text{ cm}^{-1}$ and $\epsilon_{572} = 11.4 \text{ mM}^{-1} \text{ cm}^{-1}$).³⁵ The concentrations of the Hb solutions are always expressed per heme.

Purified metMb solutions were prepared as described previously.³⁶ Concentrated MbFe(II)NO stock solutions were prepared via reductive nitrosylation under alkaline conditions (reaction 1).³⁷



Briefly, an alkaline concentrated metMb solution (500–800 μM in a 0.1 M phosphate buffer pH 8.6) was first saturated with Ar by

- (30) Latal, P.; Kissner, R.; Bohle, D. S.; Koppenol, W. H. *Inorg. Chem.* **2004**, *43*, 6519–6521.
 (31) Kissner, R.; Koppenol, W. H. *Methods Enzymol.* **2005**, *396*, 61–68.
 (32) Koppenol, W. H.; Kissner, R.; Beckman, J. S. *Methods Enzymol.* **1996**, *269*, 296–302.
 (33) Herold, S.; Exner, M.; Boccini, F. *Chem. Res. Toxicol.* **2003**, *16*, 390–402.
 (34) Harned, H. S.; Bonner, F. T. *J. Am. Chem. Soc.* **1945**, *67*, 1026–1031.
 (35) Kharitonov, V. G.; Bonaventura, J.; Sharma, V. S. *Methods Enzymol.* **1996**, *269*, 39–45.
 (36) Herold, S.; Rehmann, F.-J. K. *Free Radical Biol. Med.* **2003**, *34*, 531–545.

applying alternatively a vacuum and an atmosphere of Ar to the solution for at least eight times while gently stirring. Then, to saturate the protein solution with NO•, we applied analogously a vacuum and an atmosphere of NO• for 3–4 times. The protein solution was allowed to react overnight at room temperature and was finally saturated with Ar by again applying eight cycles of a vacuum and Ar. The final concentration of the diluted MbFe(II)NO solutions used for the stopped-flow experiments was determined prior to each measurement by determining the absorbance at 547 and 579 nm ($\epsilon_{547} = 11.8 \text{ mM}^{-1} \text{ cm}^{-1}$ and $\epsilon_{579} = 10.5 \text{ mM}^{-1} \text{ cm}^{-1}$).³⁵

The HbFe(II)NO and MbFe(II)NO stock solutions were prepared freshly for each experiment. As the nitrosyl proteins were slowly oxidized by oxygen^{19,38} the solutions were diluted with a degassed buffer and always kept under Ar.

Stopped-Flow Experiments. The protein solutions were prepared by diluting the HbFe(II)NO and MbFe(II)NO stock solutions to the desired concentration with a degassed 0.1 M phosphate buffer (pH 5.6–7.3) under anaerobic conditions. To avoid oxidation of the nitrosyl forms of the proteins, ~30 mL of diluted protein solution were prepared at a time and used as fast as possible. For the experiments in the presence of CO₂, the required amount of bicarbonate was added to the diluted protein solution from a degassed bicarbonate stock solution. Peroxyntirite solutions were prepared by diluting the stock solution immediately before use with degassed 0.01 M NaOH to achieve the required concentration. In general, the protein was dissolved in a 0.1 M buffer at a pH slightly more acidic (0.2–0.6 pH units lower) than the desired final pH, which was always measured at the end of the reactions for control.

Kinetics studies of the reactions of peroxyntirite with HbFe(II)NO and with MbFe(II)NO were carried out either with a SX18MV–R or a SX17MV Applied Photophysics single-wavelength stopped-flow instrument and with an On-Line Instrument Systems Inc. stopped-flow instrument equipped with an OLIS RSM 1000 rapid scanning monochromator. The length of the cells in the three spectrophotometers is 1 cm. The mixing time of the instruments is 2–4 ms. All measurements were carried out at 20 °C.

With the Applied Photophysics instrument, kinetics traces were collected at different wavelengths between 300 and 650 nm, and the data were analyzed with Kaleidagraph, version 3.6.2. For the determination of the observed rate constants of the reaction between MbFe(II)NO and peroxyntirite, the reaction time courses were collected at 420 nm in the absence of added CO₂ and at 516 and 536 nm in its presence. For the determination of the observed rate constants of the two steps of the reaction between HbFe(II)NO and peroxyntirite, the reaction time courses were collected at 516/517 and 602 nm in the absence of added CO₂ and at 582/583 and 560 nm in its presence. In all cases, the results of the fits of the traces (averages of at least 10 single traces) from at least five experiments were averaged to obtain each observed rate constant, given with the corresponding standard error. Care was taken that the absolute absorbance of the reaction mixture was not higher than one absorbance unit. Alternatively, the observed rate constants were determined by singular-value decomposition and global analysis of the spectral data collected with the OLIS instrument.

Kinetics studies of the nitrite-catalyzed peroxyntirite-mediated oxidation of HbFe(II)NO were carried out by adding the required amounts of nitrite from a degassed stock solution (pH 9.5) to the degassed diluted peroxyntirite solution. In most cases, the observed

- (37) Hoshino, M.; Maeda, M.; Konishi, R.; Seki, H.; Ford, P. C. *J. Am. Chem. Soc.* **1996**, *118*, 5702–5707.
 (38) Arnold, E. V.; Bohle, D. S. *Methods Enzymol.* **1996**, *269*, 41–55.

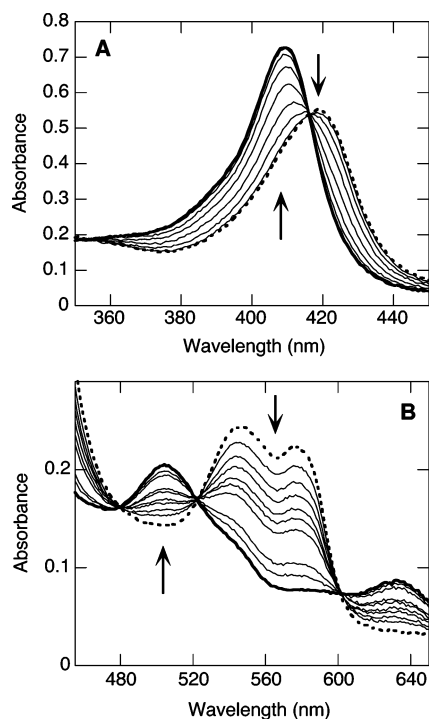


Figure 1. Rapid-scan UV/vis spectra of the reaction between MbFe(II)NO and peroxynitrite. (A) $\sim 4 \mu\text{M}$ MbFe(II)NO and $161 \mu\text{M}$ peroxynitrite, in a 0.05 M phosphate buffer at pH 7.0 and 20°C . The traces depicted were recorded each at 100 ms. (B) $\sim 20 \mu\text{M}$ MbFe(II)NO and $156 \mu\text{M}$ peroxynitrite, in a 0.05 M phosphate buffer at pH 7.2 and 20°C . The traces depicted were recorded 20, 40, 60, 80, 100, 120, 160, 200, 240, and 480 ms after mixing. In both parts, the spectrum of MbFe(II)NO is shown as a dotted bold line, whereas the final spectrum of metMb is shown as a bold line.

rate constants were determined by singular-value decomposition and global analysis of the spectral data collected with the OLIS instrument.

Kinetics of the Nitrite-Mediated Oxidation of HbFe(II)NO and of MbFe(II)NO. Kinetics studies of the reaction of nitrite with HbFe(II)NO/MbFe(II)NO were carried out with an Analytic Jena Specord 200 spectrometer. The spectra were collected in the range 450–650 nm. The HbFe(II)NO [or MbFe(II)NO] solution was first transferred in an Ar-filled Hellma quartz cell for anaerobic applications, and the reaction was started by adding the required amount of nitrite from a degassed nitrite stock solution (pH 7.0–7.3).

Results

Rapid-Scan UV/vis Spectroscopic Studies of the Reaction of Peroxynitrite with MbFe(II)NO in the Absence of Carbon Dioxide. Preliminary studies of the reaction of peroxynitrite with nitrosylmyoglobin [MbFe(II)NO] showed that it apparently proceeds in one step (Figure 1), in contrast to the corresponding reaction with nitrosylhemoglobin [HbFe(II)NO].²¹ Recent studies showed that, in the first step, peroxynitrite oxidizes HbFe(II)NO to HbFe(III)NO, from which, in the second step, NO^\bullet dissociates to form metHb.²¹ As shown in Figure 1A, the addition of an excess of peroxynitrite to MbFe(II)NO led to the shift of the maximum of the Soret band from 419 nm [characteristic maximum for MbFe(II)NO, dotted bold line] to 408 nm (characteristic maximum for metMb, bold line), with an isosbestic point at 416 nm. In the visible region of the spectrum (Figure 1B),

the absorbance changes also corresponded to the transformation of MbFe(II)NO to metMb. Indeed, the first spectrum (dotted bold line in Figure 1B) is characteristic for MbFe(II)NO ($\lambda_{\text{max}} = 547$ and 579 nm),³⁵ and the last one (bold line in Figure 1B) is that of metMb ($\lambda_{\text{max}} = 502$ and 630 nm).³⁹ Also in the visible part of the spectrum, one set of isosbestic points was clearly visible at 480, 522, and 602 nm. The absorbance changes and the presence of only one set of isosbestic points suggest that under our experimental conditions the observed rate of NO^\bullet dissociation from MbFe(III)NO must be larger than that of the peroxynitrite-mediated oxidation of MbFe(II)NO to MbFe(III)NO.

Interestingly, hydrogen peroxide, another biologically relevant oxidizing agent, cannot oxidize either HbFe(II)NO or MbFe(II)NO. In fact, the addition of a large excess of H_2O_2 (up to 1 M) leaves the spectra of HbFe(II)NO and MbFe(II)NO unchanged for at least 1 min (data not shown).

pH-Dependence of the Oxidation Rate of MbFe(II)NO by Peroxynitrite in the Absence of Carbon Dioxide. The kinetics of the reaction of MbFe(II)NO with peroxynitrite were studied at pH 6.3, 7.5, and 8.3 (at 20°C). In all of our experiments, peroxynitrite was present at least in 10-fold excess to maintain pseudo-first-order conditions. The reaction time courses, measured at 420 nm, were fitted to a single-exponential expression (data not shown). Depending on the pH and on the peroxynitrite concentration, in some cases, the kinetics traces showed an apparent lag phase or a slight increase followed by a larger decrease in absorbance. In these cases, the reaction time courses were fitted to a single-exponential expression by omitting the beginning. This curve shape could be satisfactorily simulated (see discussion below) and arises from the strong similarity of the absorbance spectra of MbFe(II)NO ($\epsilon_{420} = 132 \text{ mM}^{-1} \text{ cm}^{-1}$)³⁵ and MbFe(III)NO ($\epsilon_{421} = 150 \text{ mM}^{-1} \text{ cm}^{-1}$).⁴⁰ Moreover, at the beginning of the reaction, the absorbance decrease due to the conversion of MbFe(II)NO to metMb is partly compensated by the increase in absorbance arising from the conversion of MbFe(II)NO to MbFe(III)NO. At a given pH, the length of this lag phase decreased with increasing peroxynitrite concentration because the amount of peroxynitrite influences the rate of the first reaction step but not that of NO^\bullet dissociation from MbFe(III)NO.

As shown in Figure 2A, at all pH values studied, the observed rate constants for the peroxynitrite-mediated oxidation of MbFe(II)NO increased with increasing peroxynitrite concentration but reached a saturation point at very high peroxynitrite concentrations. This trend was particularly well-visible for the reaction carried out at pH 6.3 (Figure 2A). The peroxynitrite concentration required to reach saturation increased with increasing pH. These observations indicate that at low peroxynitrite concentrations the rate-determining step of the reaction is the oxidation of MbFe(II)NO, whereas in the presence of significantly larger amounts of peroxynitrite, the dissociation of NO^\bullet from MbFe(III)NO becomes rate-determining.

(39) Antonini, E.; Brunori, M. *Hemoglobin and Myoglobin in Their Reactions with Ligands*; North-Holland, Amsterdam, 1971.

(40) Addison, A. W.; Stephanos, J. J. *Biochemistry* **1986**, *25*, 4104–4113.

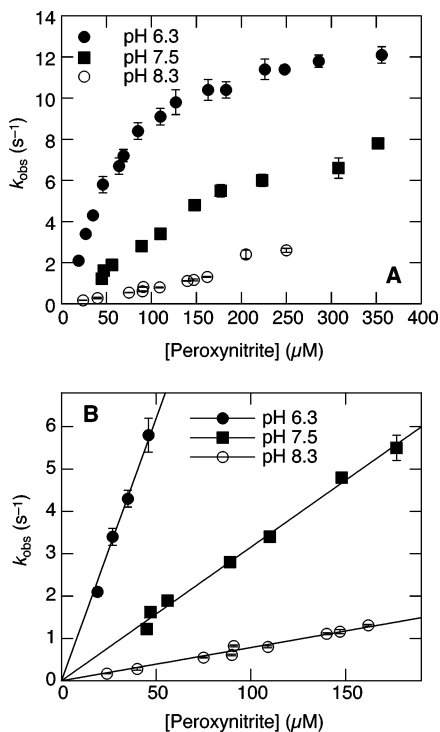


Figure 2. Plots of k_{obs} versus peroxy-nitrite concentration for the peroxy-nitrite-mediated oxidation of MbFe(II)NO ($2 \mu\text{M}$) in a 0.05 M phosphate buffer at pH 6.3, 7.5, and 8.3 (at $20 \text{ }^\circ\text{C}$). In B, fits of the linear part of the three plots shown in A are given. The second-order rate constants resulting from the linear fits depicted are summarized in Table 1.

Table 1. pH-Dependence of the Second-Order Rate Constants ($\text{M}^{-1} \text{s}^{-1}$) of the Peroxynitrite-Mediated Oxidation of MbFe(II)NO in the Absence and in the Presence of CO_2 , Obtained at $20 \text{ }^\circ\text{C}$

$[\text{CO}_2]$ (mM)	pH	MbFe(II)NO \rightarrow MbFe(III)NO
0	6.3	$(1.2 \pm 0.1) \times 10^5$
1.2	6.3	$(7 \pm 1) \times 10^4$
0	7.5	$(3.1 \pm 0.1) \times 10^4$
1.2	7.0	$(1.7 \pm 0.1) \times 10^5$
0	8.3	$(7.8 \pm 0.2) \times 10^3$
1.2	7.7	$(1.9 \pm 0.1) \times 10^5$

To get the second-order rate constant of the first reaction step, we fitted the linear part of the plots of the observed rate constants versus the peroxy-nitrite concentration (Figure 2B). The values, obtained from the linear fits and given in Table 1, decreased with increasing pH. The observed pH-dependence suggests that HOONO ($\text{p}K_{\text{a}} = 6.8$)⁴¹ or the products of its decomposition are the species that react with MbFe(II)NO.

The reaction between peroxy-nitrite and MbFe(II)NO was also studied by following the absorbance changes at 302 nm, the absorbance maximum of peroxy-nitrite. At pH 7.1, in the presence of 3–11 μM MbFe(II)NO, we first observed a small rapid absorbance decrease due to the stoichiometric reaction of peroxy-nitrite (100 μM) with MbFe(II)NO and possibly also arising from the absorbance changes of the protein spectrum upon the oxidation of MbFe(II)NO to metMb. Over a longer time scale, a further absorbance decrease reflected the disappearance of the remaining peroxy-nitrite, which decayed with an observed rate constant only slightly larger than that measured in the absence of the protein. The observed rate constant for this decay process increased

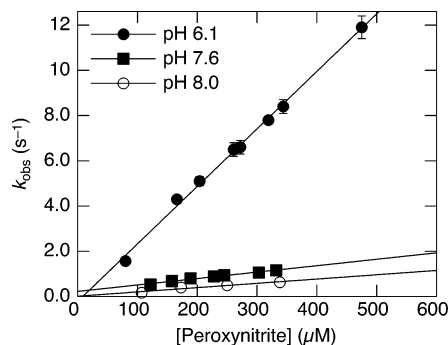


Figure 3. Plots of k_{obs} versus peroxy-nitrite concentration for the peroxy-nitrite-mediated oxidation of HbFe(II)NO ($10 \mu\text{M}$) in a 0.05 M phosphate buffer at pH 6.1, 7.6, and 8.0 (at $20 \text{ }^\circ\text{C}$). The second-order rate constants resulting from the linear fits depicted are summarized in Table 2.

Table 2. pH-Dependence of the Second-Order Rate Constants ($\text{M}^{-1} \text{s}^{-1}$) of the Peroxynitrite-Mediated Oxidation of HbFe(II)NO in the Absence and in the Presence of CO_2 , Obtained at $20 \text{ }^\circ\text{C}$

$[\text{CO}_2]$ (mM)	pH	HbFe(II)NO \rightarrow HbFe(III)NO
0	6.1	$(2.5 \pm 0.1) \times 10^4$
1.2	6.2	$(6.2 \pm 0.6) \times 10^4$
0	7.6	$(2.8 \pm 0.1) \times 10^3$
0	7.2 ^a	$(6.1 \pm 0.3) \times 10^3$
1.2	7.2	$(5.8 \pm 0.3) \times 10^4$
0	8.0	$(1.9 \pm 0.5) \times 10^3$
1.2	7.8	$(5.3 \pm 0.2) \times 10^4$

^a Ref 21.

linearly with increasing MbFe(II)NO concentration (data not shown). The catalytic rate constant obtained from the linear fit was $(1.9 \pm 0.4) \times 10^4 \text{ M}^{-1} \text{ s}^{-1}$, a value very close to that measured for the catalytic rate constant of the metMb-catalyzed decay of peroxy-nitrite [$(1.2 \pm 0.1) \times 10^4 \text{ M}^{-1} \text{ s}^{-1}$, at pH 7.5 and $20 \text{ }^\circ\text{C}$].⁴² Taken together, these observations suggest that metMb formed from the peroxy-nitrite-mediated oxidation of MbFe(II)NO is responsible for the observed slight acceleration of the decay of peroxy-nitrite.

pH-Dependence of the Oxidation Rate of HbFe(II)NO by Peroxynitrite in the Absence of Carbon Dioxide. The kinetics of the reaction of HbFe(II)NO with peroxy-nitrite were studied at pH 6.1, 7.6, and 8.0 (at $20 \text{ }^\circ\text{C}$). Also for the reaction with Hb, in all of our experiments, peroxy-nitrite was present at least in 10-fold excess to maintain pseudo-first-order conditions. As mentioned above,²¹ for the reaction between peroxy-nitrite and HbFe(II)NO, the two reaction steps could be observed separately. The reaction time courses for the two reaction steps were measured at 517 and 602 nm, respectively. For both steps, the reaction time courses could be fitted to a single-exponential expression (data not shown). The observed rate constants for the first reaction step depended linearly on the peroxy-nitrite concentration (Figure 3), and the second-order rate constants given in Table 2 were obtained from the linear fits of the plots.

As shown in Figure 3, also for the reaction with Hb, the values of the second-order rate constants decreased with increasing pH (Table 2). For all pH values measured, the

(41) Kissner, R.; Nauser, T.; Bugnon, P.; Lye, P. G.; Koppenol, W. H. *Chem. Res. Toxicol.* **1997**, *10*, 1285–1292.

(42) Herold, S.; Matsui, T.; Watanabe, Y. *J. Am. Chem. Soc.* **2001**, *123*, 4085–4086.

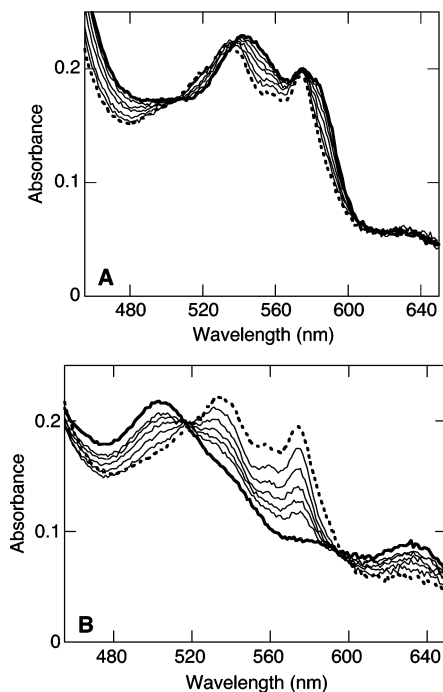


Figure 4. Rapid-scan UV/vis spectra of the reaction of MbFe(II)NO ($\sim 20 \mu\text{M}$) with peroxyntirite ($175 \mu\text{M}$) in the presence of CO_2 (1.2 mM), in a 0.05 M phosphate buffer at pH 7.4 and 20°C . (A) Oxidation of MbFe(II)NO (bold line) to MbFe(III)NO (bold dotted line): the traces depicted were recorded 3, 6, 9, 15, 18, and 25 ms after mixing. (B) The dissociation of NO^* from MbFe(III)NO (bold dotted line) generates metMb (bold line). The traces depicted were recorded 25, 50, 75, 100, 125, 150, and 350 ms after mixing.

values of the observed as well as the second-order rate constants for the reaction of peroxyntirite with MbFe(II)NO were always larger than those with HbFe(II)NO (Tables 1 and 2).⁴³

As expected, the values of the observed rate constants for the second reaction step, which is NO^* dissociation from HbFe(III)NO, did not depend on the peroxyntirite concentration. The rates slightly decreased with increasing pH: $1.6 \pm 0.1 \text{ s}^{-1}$ (pH 6.1), $1.1 \pm 0.1 \text{ s}^{-1}$ (pH 7.6), and $0.7 \pm 0.1 \text{ s}^{-1}$ (pH 8.0).

Rapid-Scan UV/vis Spectroscopic Studies of the Reaction of Peroxyntirite with MbFe(II)NO in the Presence of 1.2 mM Carbon Dioxide. Preliminary studies of the reaction of peroxyntirite with nitrosylmyoglobin [MbFe(II)NO] showed that in the presence of 1.2 mM CO_2 the two reaction steps could be distinguished (Figure 4), in analogy to the corresponding reaction with nitrosylhemoglobin [HbFe(II)NO] under similar conditions.²¹ As shown in Figure 4A, the reaction of ca. $20 \mu\text{M}$ MbFe(II)NO with an excess of peroxyntirite ($175 \mu\text{M}$) led first to the shift of the absorbance maxima characteristic for MbFe(II)NO (bold line, $\lambda_{\text{max}} = 547$ and 579 nm)³⁵ to those typical for

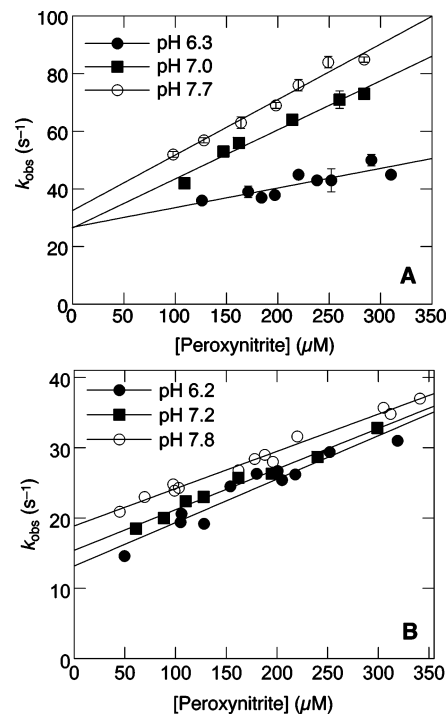


Figure 5. Plots of k_{obs} versus peroxyntirite concentration for the peroxyntirite-mediated oxidation of (A) MbFe(II)NO ($10 \mu\text{M}$) and (B) HbFe(II)NO ($10 \mu\text{M}$) in the presence of CO_2 (1.2 mM), in a 0.05 M phosphate buffer at 20°C . The second-order rate constants resulting from the linear fits depicted are summarized in Tables 1 and 2.

MbFe(III)NO (bold dotted line, $\lambda_{\text{max}} = 532$ and 574 nm).⁴⁰ In the second reaction step (Figure 4B), the dissociation of NO^* led to the appearance of the absorbance maxima characteristic for metMb (bold line, $\lambda_{\text{max}} = 502$ and 630 nm).³⁹ Two sets of isosbestic points are distinguishable for the two reaction steps, $505/536 \text{ nm}$ and $516/593 \text{ nm}$, for the first and the second steps, respectively. Taken together, these observations indicate that, in the presence of 1.2 mM CO_2 , the mechanism of the reaction between peroxyntirite and MbFe(II)NO is identical to that in the absence of carbon dioxide. Moreover, the oxidation proceeds at a faster rate, and thus, the two reaction steps are distinguishable.

pH-Dependence of the Second-Order Rate Constant of the Peroxyntirite-Mediated Oxidation of MbFe(II)NO and HbFe(II)NO in the Presence of 1.2 mM Carbon Dioxide. The kinetics of the reaction of MbFe(II)NO with peroxyntirite in the presence of 1.2 mM CO_2 were studied at pH 6.3, 7.0, and 7.7 (at 20°C). Also for the reactions in the presence of CO_2 in all our experiments, peroxyntirite was present at least in 10-fold excess to maintain pseudo-first-order conditions. As mentioned above, under these conditions, the two reaction steps could be observed separately and were studied at two different wavelengths. The reaction time courses for the peroxyntirite-mediated oxidation of MbFe(II)NO to MbFe(III)NO were measured at 516 nm , one of the isosbestic points of the NO^* dissociation from MbFe(III)NO (Figure 4). The observed rate constant for NO^* dissociation from MbFe(III)NO was determined by fitting the exponential absorbance decay at 536 nm , one of the isosbestic points of the oxidation of MbFe(II)NO to MbFe(III)NO.

(43) As the pH values of different preparations of the peroxyntirite solutions are not always identical, it is very difficult to predict the final pH at which the reactions take place. Thus, the pH values at which the kinetics studies were carried out for the two proteins were not identical but varied within 0.1 and 0.3 pH units. However, the difference between the values of the second-order rate constants for the reaction with Mb and that with Hb is unquestionable, mostly 1 order of magnitude.

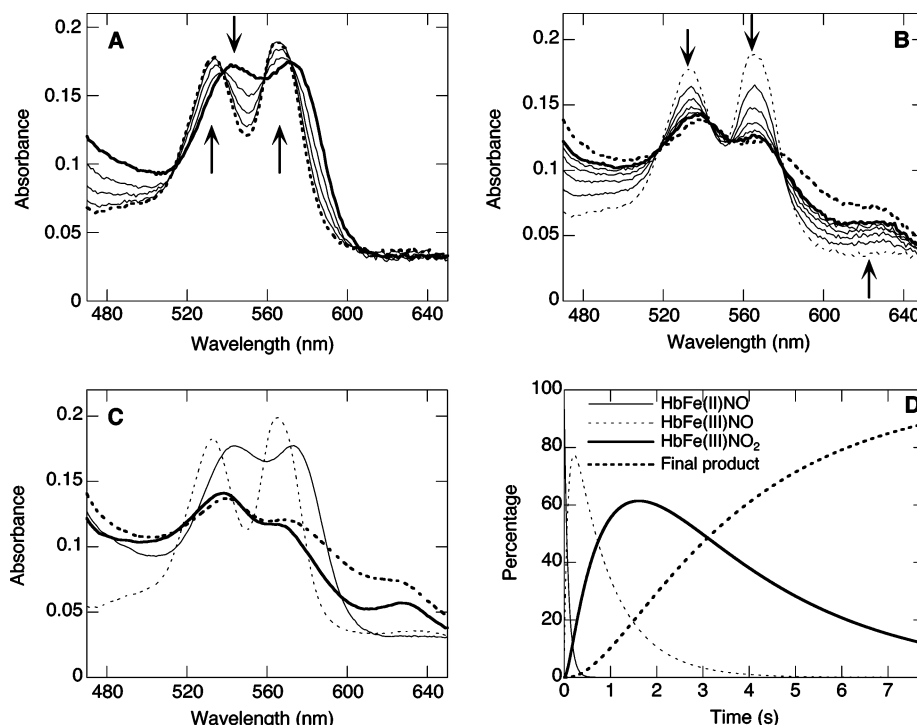


Figure 6. Rapid-scan UV/vis spectra of the nitrite-catalyzed reaction between HbFe(II)NO (14 μM) and peroxyntirite (400 μM) in a 0.05 M phosphate buffer at pH 7.0 and 20 $^{\circ}\text{C}$, $[\text{NO}_2^-] = 175 \text{ mM}$. Absorbance spectra were collected every millisecond, but to improve the signal-to-noise ratio, each curve shown represents the average of two measured curves. (A) Oxidation of HbFe(II)NO (bold line) to HbFe(III)NO (bold dotted line): the traces depicted were recorded every 40 ms up to 160 ms. (B) The dissociation of NO[•] from HbFe(III)NO (dotted line) and the binding of nitrite to metHb generates HbFe(III)NO₂ (bold line, $\sim 2.2 \text{ s}$). The traces depicted were recorded every 400 ms. The dotted bold line represents the final spectrum after a total of 7.8 s. (C) The three species obtained from singular-value decomposition and global analysis of the data from parts A and B. The data were fitted to a three-exponential expression (A \rightarrow B \rightarrow C \rightarrow D), and the values of the three observed rate constants obtained are $11.6 \pm 0.2 \text{ s}^{-1}$, $1.2 \pm 0.1 \text{ s}^{-1}$, and $0.31 \pm 0.06 \text{ s}^{-1}$, respectively. (D) Time courses for the four species involved (see legend) obtained from singular-value decomposition and global analysis of the data from parts A and B.

A comparison of Figures 2B and 5A shows that, in the presence of 1.2 mM CO₂, all observed rate constants for the reaction between peroxyntirite and MbFe(II)NO were significantly higher than those measured in its absence at the same peroxyntirite concentration. At all pH values studied, the observed rate constants obtained from the exponential fits of the kinetics traces depended linearly on the peroxyntirite concentration (Figure 5A). Both the values of the observed rate constants and those of the second-order rate constants, obtained from the linear fits of the plots, increased with increasing pH, in particular, between pH 6.3 and 7.0 (Table 1). Carbon dioxide is known to rapidly react with ONOO⁻ to yield the adduct ONOOCO₂⁻, which partly decomposes to CO₃^{•-} and NO₂[•].^{44–46} We have previously shown that both radicals can oxidize the iron center in MbFe(II)NO.²⁷ Thus, the observed pH-dependence of the second-order rate constants suggests that these two radicals may be responsible for the oxidation of MbFe(II)NO upon the addition of peroxyntirite in the presence of 1.2 mM CO₂.

As expected, the values of the observed rate constants for NO[•] dissociation from MbFe(III)NO, the second reaction step, did not depend on the peroxyntirite concentration. Moreover, the rates were essentially pH-independent: $10 \pm$

2 s^{-1} (pH 6.3), $10.8 \pm 0.3 \text{ s}^{-1}$ (pH 7.0), and $9.9 \pm 0.2 \text{ s}^{-1}$ (pH 7.7).

Similar studies were also carried out with HbFe(II)NO. The kinetics of the reaction of HbFe(II)NO with peroxyntirite in the presence of 1.2 mM CO₂ were studied at pH 6.2, 7.2, and 7.8 (at 20 $^{\circ}\text{C}$). The reaction time courses for the peroxyntirite-mediated oxidation of HbFe(II)NO were measured at 582/583 nm, one of the isosbestic points of the NO[•] dissociation from HbFe(III)NO.²¹ The observed rate constant for NO[•] dissociation from HbFe(III)NO was determined by fitting the exponential absorbance decay at 560 nm, one of the isosbestic points of the oxidation of HbFe(II)NO to HbFe(III)NO.

As shown in Figure 5B, at all pH values studied, the observed rate constants obtained from the exponential fits of the kinetics traces depended linearly on the peroxyntirite concentration. In analogy to the reaction with MbFe(II)NO, the values of the observed rate constants were significantly higher than those measured under similar conditions in the absence of CO₂ and, moreover, slightly increased with increasing pH. In contrast, no big pH-dependence was observed among the values of the second-order rate constants obtained from the linear fits of the plots (Table 2). Also in the presence of 1.2 mM CO₂, for all pH values measured, the values of the observed and the second-order rate constants for the reaction of peroxyntirite with MbFe(II)NO were always larger than those for the reaction with HbFe(II)NO (Tables 1 and 2). As expected, the values of the observed

(44) Meli, R.; Nauser, T.; Koppenol, W. H. *Helv. Chim. Acta* **1999**, *82*, 722–725.

(45) Denicola, A.; Freeman, B. A.; Trujillo, M.; Radi, R. *Arch. Biochem. Biophys.* **1996**, *333*, 49–58.

(46) Lyman, S. V.; Hurst, J. K. *J. Am. Chem. Soc.* **1995**, *117*, 8867–8868.

rate constants for NO^\bullet dissociation from HbFe(III)NO did not depend on the peroxyxynitrite concentration and were comparable to those measured in the absence of CO_2 : $1.7 \pm 0.1 \text{ s}^{-1}$ (pH 6.2), $1.2 \pm 0.1 \text{ s}^{-1}$ (pH 7.2), and $1.0 \pm 0.1 \text{ s}^{-1}$ (pH 7.8).

Nitrite-Catalyzed Peroxyxynitrite-Mediated Oxidation of HbFe(II)NO . As our peroxyxynitrite solutions all contained small amounts of nitrite contaminations (up to 10% of the peroxyxynitrite concentration),³⁰ we investigated the influence of added nitrite on the rate and the mechanism of HbFe(II)NO oxidation by peroxyxynitrite. Preliminary results showed that in order to see an effect nitrite had to be present in large quantities (in the tens to hundreds of millimoles range). Thus, the small impurities present in the peroxyxynitrite solution did not affect our studies.

As shown in Figure 6, in the presence of 175 mM nitrite, the peroxyxynitrite-mediated oxidation of HbFe(II)NO proceeded according to the same mechanism as in its absence. The absorbance maxima characteristic for HbFe(II)NO (bold line in Figure 6A) shifted to those typical for HbFe(III)NO (bold dotted line in Figure 6A). In the presence of a large excess of nitrite, the dissociation of NO^\bullet from HbFe(III)NO was followed by the immediate binding of nitrite to metHb. Thus, the bold spectrum observed in Figure 6B is that of HbFe(III)NO_2 ($\lambda_{\text{max}} = 538$ and 567 nm).³⁶ As NO^\bullet dissociation is the rate-determining step of these two processes, only one set of isosbestic points is distinguishable in Figure 6B (at 518, 543, 553, and 578 nm). Over a longer time scale, HbFe(III)NO_2 decomposed to generate an unidentified Hb species with the dotted bold spectrum shown in Figure 6B.⁴⁷ The analysis of the spectra with singular-value decomposition/global analysis demonstrated that the spectral changes follow a three-exponential process and are indicative of the formation of HbFe(III)NO and HbFe(III)NO_2 as intermediates (Figure 6C). The observed rate constants for the first two reaction steps were determined by global analysis of the rapid-scan stopped-flow spectrophotometric data (Figure 6D). As shown in Figure 7A, the observed rate constants for the first reaction step, the oxidation of HbFe(II)NO by $400 \mu\text{M}$ peroxyxynitrite, depended linearly on the amount of nitrite added. The catalytic rate constant obtained from the linear fit of the plot increased with decreasing pH (Figure 7A and Table 3). This observation suggests that nitrite interacts with HOONO to produce an oxidizing agent more active than peroxyxynitrite.

At pH 6.2, we also studied the influence of the peroxyxynitrite concentration on the catalytic rate constant. As shown in Figure 7B, in the presence of only $200 \mu\text{M}$ peroxyxynitrite, the values of the observed rate constants were lower, but also the value of the catalytic rate constant was slightly lower (Table 3).

(47) The conversion of HbFe(III)NO_2 to the unidentified final Hb species may be mediated by peroxyxynitrite. Indeed, under the conditions of this experiment, peroxyxynitrite decays within ca. 20 s and is thus still present in high concentration when HbFe(II)NO is completely converted to HbFe(III)NO_2 (ca. 1.5 s after mixing, see Figure 6). Because of the high concentrations of peroxyxynitrite and nitrite used for this experiment, the unidentified Hb species will not be formed *in vivo*. Its characterization is outside the scope of this work.

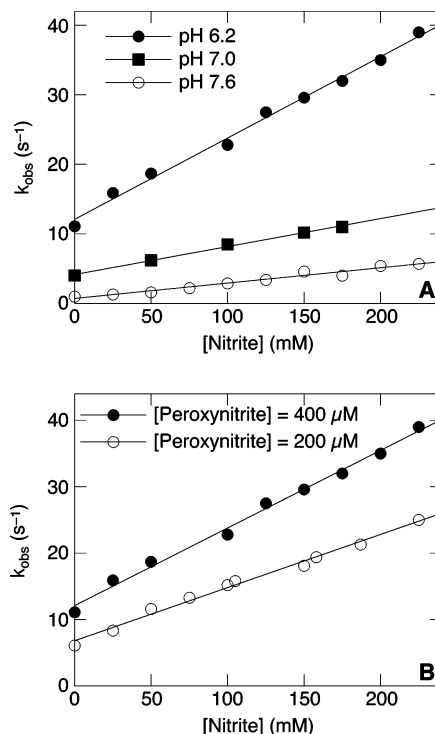


Figure 7. Plots of k_{obs} versus nitrite concentration for the nitrite-catalyzed reaction between peroxyxynitrite and HbFe(II)NO . (A) Reaction of $\sim 14 \mu\text{M}$ HbFe(II)NO with $400 \mu\text{M}$ peroxyxynitrite in a 0.05 M phosphate buffer at pH 6.2, 7.0, and 7.6 (at 20°C). (B) Comparison of the catalytic effect of nitrite on the reaction of $\sim 14 \mu\text{M}$ HbFe(II)NO with 200 or $400 \mu\text{M}$ peroxyxynitrite in a 0.05 M phosphate buffer at pH 6.2 and 20°C . The catalytic rate constants resulting from the linear fits depicted are summarized in Table 3.

Table 3. pH-Dependence of the Catalytic Rate Constants ($\text{M}^{-1} \text{ s}^{-1}$) and the NO^\bullet Dissociation Constants (s^{-1}) of the Nitrite-Catalyzed Oxidation of $\sim 14 \mu\text{M}$ HbFe(II)NO by $400 \mu\text{M}$ Peroxyxynitrite in the Absence of CO_2 , Obtained at 20°C

pH	$\text{HbFe(II)NO} \rightarrow \text{HbFe(III)NO}$	$\text{HbFe(III)NO} \rightarrow \text{HbFe(III)NO}_2$
6.2	117 ± 4	1.6 ± 0.1
6.2 ^a	80 ± 3	1.6 ± 0.2
7.0	40 ± 2	1.2 ± 0.1
7.6	22 ± 1	1.0 ± 0.1

^a Reaction with $200 \mu\text{M}$ peroxyxynitrite.

Finally, as expected, the values of the observed rate constants for NO^\bullet dissociation from HbFe(III)NO did not depend on the nitrite concentration and were comparable to those measured in the absence of nitrite: $1.6 \pm 0.2 \text{ s}^{-1}$ (pH 6.2), $1.2 \pm 0.1 \text{ s}^{-1}$ (pH 7.0), and $1.0 \pm 0.1 \text{ s}^{-1}$ (pH 7.6).

Kinetics Studies of the Nitrite-Mediated Oxidation of HbFe(II)NO . The reaction between HbFe(II)NO and nitrite was followed by UV/vis spectroscopy at pH 7.0. As shown in Figure 8A, the addition of a large excess of nitrite (ca. 8000 equiv) led to the slow oxidation of HbFe(II)NO to HbFe(III)NO . As discussed above for the nitrite-catalyzed reaction between peroxyxynitrite and HbFe(II)NO , in the presence of large quantities of nitrite, the dissociation of NO^\bullet from HbFe(III)NO , the second reaction step, is followed by the rapid binding of nitrite to metHb. Thus, the last spectrum shown in Figure 8A is again that of HbFe(III)NO_2 . Careful analysis of the spectral changes depicted in Figure 8A revealed that the oxidation of HbFe(II)NO occurred with one set of isosbestic points at 521 and 597 nm . Nevertheless,

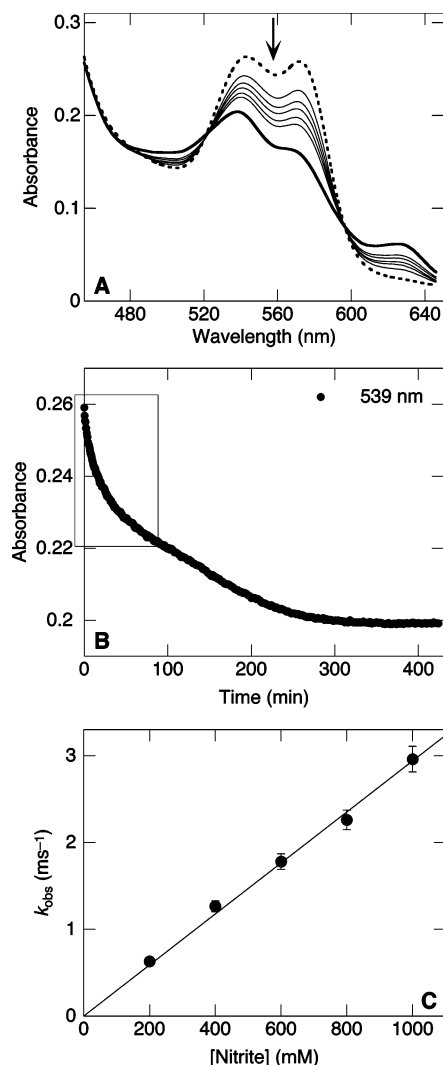


Figure 8. (A) UV/vis spectra of the reaction between nitrite (175 mM) and HbFe(II)NO (22 μM) in a 0.1 M phosphate buffer at pH 7.0 and 20 °C. The traces depicted were recorded 15, 30, 60, 90, 120, and 240 min after mixing. (B) Reaction time course of the data set shown in A, extracted at 539 nm. (C) Plot of k_{obs} versus nitrite concentration for the reaction between HbFe(II)NO (~20 μM) and nitrite in a 0.1 M phosphate buffer at pH 7.0 and 20 °C. The observed rate constants were obtained by fitting the first exponential decay of the traces extracted at 539 nm (see box in part B). The second-order rate constant resulting from the linear fit depicted is given in the text.

kinetics traces extracted at different wavelengths showed that the mechanism of the reaction is more complex. Figure 8B shows a typical example of the reaction time course at 539 nm. To get the order of magnitude of the second-order rate constant of the reaction between nitrite and HbFe(II)NO, we fitted the first part of the reaction time courses (see box in Figure 8B) with a single-exponential expression. We found that the observed rate constants depended linearly on the nitrite concentration (Figure 8C), and the second-order rate constant obtained from the linear fit was $(2.9 \pm 0.1) \times 10^{-3} \text{ M}^{-1} \text{ s}^{-1}$.

Discussion

Nitrosylhemoglobin [HbFe(II)NO] has been proposed to represent a stabilized form of NO• which is generated in the red blood cells and which may lead to the recovery of NO•

bioactivity after the release of NO• in the capillaries. Support for this hypothesis is, among other things, the observation of a higher HbFe(II)NO concentration in venous versus arterial blood of congestive heart failure patients⁴⁸ and in a rat model of endotoxemic sepsis.⁴⁹ We have previously shown that peroxyntirite, a biologically relevant oxidizing and nitrating species produced by the nearly diffusion-limited reaction between NO• and O₂^{•-},^{50,51} can oxidize the iron center of HbFe(II)NO by an outer-sphere mechanism to produce HbFe(III)NO from which NO• is released to generate metHb.²¹ The stopped-flow studies presented in this paper show that a similar reaction occurs also between peroxyntirite and MbFe(II)NO. However, as the rate of dissociation of NO• from MbFe(III)NO is 1 order of magnitude larger than that from HbFe(III)NO, the reaction between peroxyntirite and MbFe(II)NO apparently takes place in one step. For both proteins, the pH-dependence of the second-order rate constant suggests that HOONO is responsible for the oxidation of the iron centers (reaction 2 in Table 4). Indeed, the kinetics traces for the reaction with MbFe(II)NO could be simulated³³ satisfactorily with reactions 1–8 of Table 4. We have recently shown that NO₂[•] also oxidizes HbFe(II)NO and MbFe(II)NO to their corresponding iron(III) forms by an outer-sphere mechanism, and we have determined that the second-order rate constants for these reactions are on the order of 10⁷ M⁻¹ s⁻¹.²⁷ However, NO₂[•] produced from reaction 2 (Table 4) does not contribute significantly to the oxidation of MbFe(II)NO in the presence of peroxyntirite. Indeed, the addition of reaction 9 (Table 4) did not influence the simulation results.

At all pH values studied, the second-order rate constants for the reaction with Mb are larger than those for the reaction with Hb. This difference may reflect the slightly higher value of the reduction potential estimated for HbFe(III)NO [$E^\circ(\text{HbFe(III)NO}/\text{HbFe(II)NO}) = 0.55 \text{ V}$] compared to that for MbFe(III)NO [$E^\circ(\text{MbFe(III)NO}/\text{MbFe(II)NO}) = 0.47 \text{ V}$].⁵²

We have previously shown that peroxyntirite reacts with various forms of Mb and Hb according to different pathways. Their iron(III) forms, metMb and metHb, catalyze the isomerization of peroxyntirite to nitrate, albeit not very efficiently (at pH 7.0 and 20 °C, $k_{\text{cat}} = (2.9 \pm 0.1) \times 10^4$ and $(1.2 \pm 0.1) \times 10^4 \text{ M}^{-1} \text{ s}^{-1}$, respectively).⁵³ OxyMb and oxyHb are oxidized by an excess of peroxyntirite in a two-step reaction that leads to the formation of metMb and metHb, respectively. The oxygenated proteins are first oxidized to their ferryl forms that then are reduced by peroxyntirite to metMb and metHb.^{54,55} For both proteins

- (48) Datta, B.; Tufnell-Barrett, T.; Bleasdale, R. A.; Jones, C. J. H.; Beeton, I.; Paul, V.; Frenneaux, M.; James, P. *Circulation* **2004**, *109*, 1339–1342.
- (49) Davies, N. A.; Brealey, D. A.; Stidwill, R.; Singer, M.; Svistunenko, D. A.; Cooper, C. E. *Free Radical Biol. Med.* **2005**, *38*, 41–49.
- (50) Beckman, J. S.; Beckman, T. W.; Chen, J.; Marshall, P. A.; Freeman, B. A. *Proc. Natl. Acad. Sci. U.S.A.* **1990**, *87*, 1620–1624.
- (51) Nauser, T.; Koppenol, W. H. *J. Phys. Chem. A* **2002**, *106*, 4084–4086.
- (52) Ford, P. C.; Lorkovic, I. M. *Chem. Rev.* **2002**, *102*, 993–1018.
- (53) Herold, S.; Shivashankar, K. *Biochemistry* **2003**, *42*, 14036–14046.
- (54) Exner, M.; Herold, S. *Chem. Res. Toxicol.* **2000**, *13*, 287–293.
- (55) Boccini, F.; Herold, S. *Biochemistry* **2004**, *43*, 16393–16404.

Table 4. Summary of the Reactions and the Rate Constants Used for the Simulations

number	reaction	rate constant	ref
1	$\text{HOONO} \rightarrow \text{NO}_3^- + \text{H}^+$	$k_1 = 1.2 \text{ s}^{-1}$	67
2	$\text{MbFe(II)NO} + \text{HOONO} \rightarrow \text{MbFe(III)NO} + \text{NO}_2^*$	$k_2 = 2 \times 10^5 \text{ M}^{-1} \text{ s}^{-1}$	this work
3	$\text{MbFe(III)NO} + \text{H}_2\text{O} \rightleftharpoons \text{MbFe(III)OH}_2 + \text{NO}^*$	$k_3 = 10 \text{ s}^{-1}$	68
4	$\text{NO}_2^* + \text{NO}^* \rightleftharpoons \text{N}_2\text{O}_3$	$k_{-3} = 1.9 \times 10^5 \text{ M}^{-1} \text{ s}^{-1}$ $k_4 = 1.1 \times 10^9 \text{ M}^{-1} \text{ s}^{-1}$ $k_{-4} = 8.1 \times 10^4 \text{ s}^{-1}$	69
5	$\text{N}_2\text{O}_3 + \text{H}_2\text{O} \rightarrow 2\text{NO}_2^- + 2\text{H}^+$	$k_5 = 9.4 \times 10^4 \text{ s}^{-1}$	70,71
6	$2\text{NO}_2^* \rightleftharpoons \text{N}_2\text{O}_4$	$k_6 = 4.5 \times 10^8 \text{ M}^{-1} \text{ s}^{-1}$ $k_{-6} = 6.9 \times 10^3 \text{ s}^{-1}$	72
7	$\text{N}_2\text{O}_4 + \text{H}_2\text{O} \rightarrow \text{NO}_3^- + \text{NO}_2^- + 2\text{H}^+$	$k_7 = 1 \times 10^3 \text{ s}^{-1}$	72
8	$\text{N}_2\text{O}_3 + \text{ONOO}^- \rightarrow 2\text{NO}_2^* + \text{NO}_2^-$	$k_8 = 3 \times 10^8 \text{ M}^{-1} \text{ s}^{-1}$	73
9	$\text{MbFe(II)NO} + \text{NO}_2^* \rightarrow \text{MbFe(III)NO} + \text{NO}_2^-$	$k_9 = 3 \times 10^7 \text{ M}^{-1} \text{ s}^{-1}$	27

and both reaction steps, the second-order rate constants are on the order of $10^4 \text{ M}^{-1} \text{ s}^{-1}$ at neutral pH and 20°C .^{54,55} All of these reactions proceed at a faster rate at lower pH, a result that suggests that, as for the oxidation of the nitrosyl form of these proteins, HOONO is the species that interacts also with the iron(III) and the oxygenated protein forms. Alternatively, for all of these reactions, it cannot be excluded that the larger second-order rate constants obtained at lower pH may be a consequence of conformational changes occurring in the protein after the protonation of histidine residues, in particular, of the distal histidine.^{56,57} The $\text{p}K_a$ values of HOONO and of the distal histidine are 6.5–6.8⁴¹ and ~ 6 ,⁵⁶ respectively. Thus, to distinguish between the two contributions, a more detailed pH-dependence study should be carried out, which, however, is outside the scope of this work.

Mechanistic studies of the reaction of peroxynitrite with MbFe(II)NO and with HbFe(II)NO showed that, for both proteins, around neutral pH and in the presence of physiologically relevant amounts of CO_2 (1.2 mM), the observed rate constants as well as the second-order rate constants were larger than those measured in its absence.⁵⁸ As expected, the addition of CO_2 does not influence the rate of NO^* dissociation from MbFe(III)NO. Thus, in the presence of 1.2 mM CO_2 , the two reaction steps were clearly distinguishable.

Carbon dioxide is probably the compound that mostly affects peroxynitrite reactivity in biological systems. The reaction between the peroxynitrite anion and CO_2 ($6 \times 10^4 \text{ M}^{-1} \text{ s}^{-1}$ at 37°C ⁴⁶ and $3 \times 10^4 \text{ M}^{-1} \text{ s}^{-1}$ at 20°C ⁴⁵) significantly reduces the lifetime of peroxynitrite in biological systems and leads to the production of 5–30% CO_3^{*-} and NO_2^* from the decomposition of the adduct ONOOCO_2^- .^{59–61} We have recently shown that both radicals can oxidize HbFe(II)NO and MbFe(II)NO to their corresponding iron(III) forms by an outer-sphere mechanism.²⁷ As the second-order

rate constants of the reactions of HbFe(II)NO and MbFe(II)NO with CO_3^{*-} ($k \approx 10^8 \text{ M}^{-1} \text{ s}^{-1}$) are 1 order of magnitude larger than those with NO_2^* ($k \approx 10^7 \text{ M}^{-1} \text{ s}^{-1}$), it is conceivable that the former radical is responsible for the observed oxidation reaction. We have previously shown that in the presence of 1.2 mM CO_2 the peroxynitrite-mediated oxidation of oxyHb (and oxyMb) to metHb (and metMb) is also dominated by reactions of the protein with CO_3^{*-} and NO_2^* .⁵⁵ The oxygenated forms of the proteins are oxidized to the corresponding iron(III) forms by CO_3^{*-} ,⁶² and NO_2^* oxidizes oxyHb to ferrylHb, which is converted to metHb by an excess of NO_2^* .⁵⁵

Interestingly, in the presence of 1.2 mM CO_2 , the pH dependencies of the second-order rate constants for the peroxynitrite-mediated oxidation of the oxygenated and nitrosyl forms of Mb and Hb follow similar patterns. Indeed, the values increase with increasing pH for the reactions of peroxynitrite with oxyMb and MbFe(II)NO as would have been predicted. Under basic conditions, larger amounts of peroxynitrite will decay through the reaction with CO_2 , producing larger amounts of $\text{CO}_3^{*-}/\text{NO}_2^*$, and thus, one would expect that the reaction becomes faster. In contrast, the second-order rate constants for the peroxynitrite-mediated oxidation of oxyHb and HbFe(II)NO do not show a clear pH-dependence. Different factors may influence the reaction rates in opposite ways: at lower pH, it has been shown that the distal histidine is protonated and swings out of the heme pocket.^{56,57} Thus, the reaction with the iron center may be facilitated. However, at lower pH, the concentration of the anion ONOO^- , the species that reacts with CO_2 , is lower. Taken together, our data suggest that these factors influence the two proteins to a different extent and thus bring about the diverse pH dependencies of the second-order rate constants.

The experiments carried out between HbFe(II)NO and peroxynitrite in the presence of an excess of nitrite, in particular, the pH-dependence of the catalytic rate constants, suggest that an adduct between nitrite and HOONO is likely to be responsible for the acceleration of the oxidation rate. A similar adduct has been proposed to be formed as an intermediate of the reaction between peroxynitrite and a large excess of nitrite.⁶³ Indeed, the assumption of the formation of a $\text{HOONO}/\text{NO}_2^-$ adduct was essential to explain the

(56) Miller, L. M.; Patel, M.; Chance, M. R. *J. Am. Chem. Soc.* **1996**, *118*, 4511–4517.

(57) Brantley, R. E., Jr.; Smerdon, S. J.; Wilkinson, A. J.; Singleton, E. W.; Olson, J. S. *J. Biol. Chem.* **1993**, *268*, 6995–7010.

(58) For the reaction with MbFe(II)NO, the second-order rate constant in the presence of CO_2 was measured at a slightly lower pH. As discussed below, the value at pH 7.5 is expected to be even larger than that at pH 7.0 (Table 1).

(59) Goldstein, S.; Czapski, G.; Lind, J.; Merényi, G. *Chem. Res. Toxicol.* **2001**, *14*, 1273–1276.

(60) Hodges, G. R.; Ingold, K. U. *J. Am. Chem. Soc.* **1999**, *121*, 10695–10701.

(61) Meli, R.; Nausser, T.; Latal, P.; Koppenol, W. H. *J. Biol. Inorg. Chem.* **2002**, *7*, 31–36.

(62) Boccini, F.; Domazou, A. S.; Herold, S. *J. Phys. Chem. A* **2004**, *5800*–5805.

kinetics and the isotopic distribution in the products of the reaction between peroxynitrite and nitrite.⁶³ Electronic structure calculations suggest that this adduct is formed from the attack of the nitrogen atom of nitrite on the oxygen atom of HOONO to which the proton is bound.⁶³

Clearly, the nitrite concentrations used for this study are extremely high (25–250 mM). Thus, despite the fact that the pK_a of nitrous acid is ~ 3.4 , HNO_2 will be present in our solutions in the micromolar range. Nitrous acid is in equilibrium with nitrosonium-like intermediates and with N_2O_3 .⁶⁴ The reactivity of N_2O_3 toward HbFe(II)NO was studied by mixing an O_2 -containing buffer solution with a NO•-containing protein solution. For both proteins, no reaction was observed (Herold, unpublished results). Under acidic conditions, nitrite can produce NO• and $\text{NO}_2^•$ from the dissociation of N_2O_3 (reaction 4 in Table 4). The rates of NO• production have been measured and simulated for various pH values.⁶⁵ On the basis of the work of Zweier and co-workers,⁶⁵ one can calculate that under the conditions of our experiments (tens to hundreds of millimoles of nitrite and pH 6.2–7.6) the rate of NO• and, thus, of $\text{NO}_2^•$ production is in the range of 0.1–0.001 $\mu\text{M s}^{-1}$. Therefore, it is not likely that the species produced by nitrous acid influence the reaction between peroxynitrite and HbFe(II)NO. Moreover, kinetics studies of the reaction between peroxynitrite and millimolar to molar concentrations of nitrite have shown that the rate of decay of peroxynitrite depends on the nitrite concentration but is essentially identical at pH 5.2 and 3.6.⁶³ This observation further supports our conclusion that HNO_2 and the products derived from its decomposition do not affect the reactivity of peroxynitrite.

Because of the very low value of the catalytic rate constant, nitrite contaminations in peroxynitrite solutions are not likely to influence the studies of the reactions between HbFe(II)NO/MbFe(II)NO and peroxynitrite. For the same reason, the catalytic effect of nitrite does not have any physiological relevance.

Interestingly, nitrite can also selectively oxidize the iron center of HbFe(II)NO and thus lead to NO• dissociation. This observation was rather unexpected, as nitrite is not a strong oxidizing agent [$E^\circ(\text{NO}_2^•/\text{NO}_2^-) = 1.04 \text{ V}$ ⁶⁶ and $E^\circ(\text{NO}_2^-/\text{NO}^\bullet) = 0.24 \text{ V}$].⁶⁷ Comparison of the standard reduction potentials suggests that nitrite should not be able to oxidize

HbFe(II)NO [$E^\circ(\text{HbFe(III)NO}/\text{HbFe(II)NO}) = 0.55 \text{ V}$].⁵² However, under our experimental conditions (neutral pH and nonstandard concentrations of the reagents), the values are different and the reaction can take place. The second-order rate constant for this process is very small ($\sim 3 \times 10^{-3} \text{ M}^{-1} \text{ s}^{-1}$). Preliminary experiments showed that MbFe(II)NO can also be oxidized by nitrite and that, in analogy to the peroxynitrite-mediated oxidation of HbFe(II)NO/MbFe(II)NO, the reaction rate is nearly 1 order of magnitude larger. Taken together, these results suggest that, also for the nitrite-mediated oxidation of the nitrosylated forms of Hb and Mb in the absence of peroxynitrite, HNO_2 and the species derived from its decomposition are not responsible for the observed reaction. Indeed, this alternative pathway would not explain the significant difference between the rate of oxidation of the two proteins, as the rate-determining step would be the formation of $\text{NO}_2^•$ from HNO_2 . Nevertheless, because of the very high nitrite concentrations and the slow reaction rates, this process is also not likely to play a role under physiological conditions.

In summary, we have shown that NO• can be released quantitatively and at a fast rate from HbFe(II)NO and MbFe(II)NO after oxidation. In contrast to H_2O_2 , peroxynitrite, both in the absence and in the presence of CO_2 , can efficiently carry out this reaction in vitro. However, because in vivo the concentrations of HbFe(II)NO and MbFe(II)NO are significantly smaller than those of oxyHb and oxyMb, it is very unlikely that the peroxynitrite-mediated oxidation of HbFe(II)NO and MbFe(II)NO has a physiological relevance, also because the rate constants for the reactions of peroxynitrite with these two forms of the proteins are all comparable.^{54,55} Under oxygen-deficient conditions, peroxynitrite will instead react with deoxyHb and deoxyMb, present in concentrations significantly higher than those of HbFe(II)NO and MbFe(II)NO. Moreover, it can be argued that it is improbable that a toxin regulates a physiologically relevant process. Nevertheless, in this work, we have shown that, in principle, NO• can be released from HbFe(II)NO and MbFe(II)NO after oxidation of the iron centers. If this is indeed the pathway followed in vivo to restore the bioactivity of NO• from HbFe(II)NO and MbFe(II)NO, the oxidant responsible for this reaction still has to be identified.

Acknowledgment. This work was supported by the ETH Zürich. We thank APEX Bioscience, Inc. for the supply of purified human hemoglobin.

IC060469G

(63) Maurer, P.; Thomas, C. F.; Kissner, R.; Rügger, H.; Greter, O.; Röthlisberger, U.; Koppenol, W. H. *J. Phys. Chem. A* **2003**, *107*, 1763–1769.

(64) Turney, T. A.; Wright, G. A. *Chem. Rev.* **1959**, *59*, 497–513.

(65) Zweier, J. L.; Samouilov, A.; Kuppasamy, P. *Biochim. Biophys. Acta* **1999**, *1411*, 250–262.

(66) Standbury, D. M. *Adv. Inorg. Chem.* **1989**, *33*, 69–138.

(67) Koppenol, W. H.; Moreno, J. J.; Pryor, W. A.; Ischiropoulos, H.; Beckman, J. S. *Chem. Res. Toxicol.* **1992**, *5*, 834–842.

(68) Hoshino, M.; Ozawa, K.; Seki, H.; Ford, P. C. *J. Am. Chem. Soc.* **1993**, *115*, 9568–9575.

(69) Grätzel, M.; Taniguchi, S.; Henglein, A. *Ber. Bunsen-Ges. Phys. Chem.* **1970**, *74*, 488–492.

(70) Goldstein, S.; Czapski, G. *J. Am. Chem. Soc.* **1996**, *118*, 3419–3425.

(71) Lewis, R. L.; Tannenbaum, S. R.; Deen, W. M. *J. Am. Chem. Soc.* **1995**, *117*, 3933–3939.

(72) Grätzel, M.; Henglein, A.; Lillie, J.; Beck, G. *Ber. Bunsen-Ges. Phys. Chem.* **1969**, *73*, 646–653.

(73) Goldstein, S.; Czapski, G.; Lind, J.; Merényi, G. *Chem. Res. Toxicol.* **1999**, *12*, 132–136.